Macroscopic Characteristics of Lane-Changing Traffic

Wen-Long Jin

On a multilane roadway, systematic lane changes can seriously disrupt traffic flow and cause capacity reductions. Therefore it is important to understand the characteristics of lane-changing traffic flow. In a previous study, a new variable, lane-changing intensity, was theoretically derived by doubling the contribution to the total density of a lane-changing vehicle during its lane-changing period, and an intensity–density relation was incorporated into the fundamental diagram to capture such bottleneck effects at the aggregate level. In this study, a new interpretation of lane-changing intensity is proposed by following Edie's definition of traffic density. Detailed studies of macroscopic characteristics of lane-changing traffic with 75 min of vehicle trajectories collected for a freeway section on I-80 near San Francisco, California, by FHWA's next-generation simulation project are presented. About 10% misindentified lane changes are excluded. For different time intervals, cell sizes, and locations, the well-definedness of the lane-changing intensity variable and the intensity–density relation are verified.

In a road network, lane-changing areas (locations where one or more streams of vehicles systematically change lanes) could constitute significant bottlenecks (*1*) and cause accidents (*2*). Therefore, it is important to understand characteristics of lane-changing traffic flow and the behaviors of lane-changing vehicles.

Several studies have examined vehicles' behaviors related to lane-changing motive, time, location, and maneuver at the microscopic level (*3–6*). Various studies have also been carried out to understand various characteristics of lane-changing traffic at the macroscopic level: the exchange of flows between lanes (*7–10*), density oscillation and instability issues (*11, 12*), and the degree of first-in-first-out violation among vehicles (*13*). Since the publication of the *Highway Capacity Manual* in 1950, many studies have considered the level of service of weaving areas, which are special lane-changing areas (*14*). A hybrid microscopic–macroscopic model was proposed to study lane-changing traffic dynamics (*15*), and a new macroscopic model was proposed (*16*) to capture lateral interactions among vehicles in the framework of a fundamental diagram (*17*). In addition to traffic density [$\rho(x, t)$], travel speed [$v(x, t)$], and flow rate [$q(x, t)$], a new variable of lane-changing intensity [$\epsilon(x, t)$] was introduced to account for the level of lane-changing activities at location x and time t. Roughly, ϵ can be considered as the ratio of vehicles' lane-changing time to their total travel time on a road section in a space–time domain. Furthermore, an intensity–density relation was hypothesized and incorporated into the fundamental diagram to study the impacts of lane-changing traffic on overall traffic flow. Some results with observed data were shown to demonstrate that such an intensity–density relationship is yet another fundamental relationship for lane-changing traffic.

In this study, a new interpretation of lane-changing intensity (*16*) by extending Edie's definition of traffic density is proposed. Detailed studies of macroscopic characteristics of lane-changing traffic based on 75 min of vehicle trajectories collected for a freeway section on I-80 by FHWA's next-generation simulation (NGSIM) project are presented. In particular, the consistency of the data sets is carefully examined to exclude misidentified lane changes caused by limitations in video transcription. For different lane-changing thresholds, time intervals, cell sizes, and locations, the well-definedness of the lane-changing intensity variable and intensity–density relation are further verified.

The rest of the paper is organized as follows. In the next section a macroscopic theory of lane-changing traffic is reviewed, and a new interpretation of lane-changing intensity is presented. In the third section, four data sets for studying real lane-changing traffic are carefully examined. Algorithms for computing aggregate lane-changing traffic characteristics are presented in the fourth section, and in the fifth section macroscopic lane-changing intensity and the corresponding fundamental diagram for various scenarios are studied. The concluding section offers a discussion of the study.

MACROSCOPIC LANE-CHANGING THEORY

Review of Macroscopic Lane-Changing Theory

A macroscopic lane-changing theory was proposed on the basis of the observation that, in congested traffic, a lane-changing vehicle impacts traffic flow in both its previous lane and its target lane (*16*). In this theory, a lane-changing movement is considered in a three-dimensional (x, y, t) space: longitudinal direction x, lateral direction y, and time t. In particular, a lane change can be described by the lane-changing period of $t \equiv t_{LC}$ and two displacements, Δx and Δy, in the x and y directions, respectively. Furthermore, the lateral displacement threshold of the lane-changing vehicle, or simply the lane-changing threshold Δy, should be at least the width of the vehicle w. In summary, a lane change can be described by the following variables:

- Previous lane and target lane;
- Lane-changing location and time in the (x, y, t) space, (x_0, y_0, t_0);

Department of Civil and Environmental Engineering, California Institute for Telecommunications and Information Technology, Institute of Transportation Studies, University of California, Irvine, 4038 Anteater Instruction and Research Building, Irvine, CA 92697-3600. wjin@uci.edu.

Transportation Research Record: Journal of the Transportation Research Board, No. 2188, Transportation Research Board of the National Academies, Washington, D.C., 2010, pp. 55–63.
DOI: 10.3141/2188-07

- Lane-changing distances and duration in the (x, y, t) space, Δx, Δy, Δt);
- Average lane-changing angle θ, where $\tan\theta = \Delta y/\Delta x$; and
- Average longitudinal speed, $v = \Delta x/\Delta t$.

Here the variables follow the following relationship:

$$t_{LC} \equiv \Delta t = \frac{\Delta_y}{v\tan\theta} \tag{1}$$

At the aggregate level, in a space–time domain ($[x_a, x_b] \times [t_a, t_b]$), lane-changing traffic can be described by the following quantities:

- Number of lane changes, N_{LC};
- Total lane-changing time, $N_{LC}t_{LC}$;
- Lane-changing traffic density, ρ_{LC}; and
- Lane-changing traffic flow rate, q_{LC}.

On the basis of the argument (*16*) that the contribution of lane-changing vehicles should be doubled during their lane-changing periods, the effective density of total traffic was defined for a lane-changing area with a width of $L = x_b - x_a$ and a time period of duration $T = t_b - t_a$:

$$\bar{\rho} = \frac{\rho_{LT} + N_{LC}t_{LC}}{LT} = \rho + \frac{N_{LC}t_{LC}}{LT} = (1+\epsilon)\rho \tag{2}$$

where a new lane-changing intensity variable, ϵ, was given by

$$\epsilon(x,t) = \frac{N_{LC}t_{LC}}{\rho_{LT}} = \frac{N_{LC}t_{LC}}{NT} \tag{3}$$

As expected, lane-changing intensity is determined by the number of lane changes, lane-changing duration, and traffic density in the lane-changing area. Thus for lane-changing traffic there are four aggregate variables: traffic density $\rho(x, t)$, travel speed $v(x, t)$, flow rate $q(x, t)$, and lane-changing intensity $\epsilon(x, t)$. In the literature the first three variables have been well-defined and can be measured; in this study, the fourth is defined in Equation 3 and is measured for real traffic, and the relationship between lane-changing intensity and traffic density under various conditions is calibrated. That is, empirical observations support the following intensity–density relationship:

$$\epsilon = E(x,\rho) \tag{4}$$

Furthermore, a modified speed–density relationship was introduced for lane-changing area $v(x, t) = V((1 + \epsilon(x, t))\rho(x, t))$, where $V(\cdot)$ is the speed–density relationship without a lane-changing effect. Therefore, with higher lane-changing intensity, the same traffic density would lead to higher effective total density and lower average speed. The fundamental diagram with lane-changing effect is then

$$q = \rho V\left((1+\epsilon)\rho\right) \tag{5}$$

On the assumption that Equation 5 is the true fundamental diagram for lane-changing traffic, the fundamental diagram without lane changing can be obtained as

$$q = Q(\bar{\rho}) = \bar{\rho}V(\bar{\rho}) = (1+\epsilon)\rho V\left((1+\epsilon)\rho\right) \tag{6}$$

Comparing Equations 6 and 5 allows an understanding of the impact of lane-changing traffic. The Lighthill–Whitham–Richards model (*18, 19*) was extended (*16*) to incorporate a lane-changing effect:

$$\frac{\partial\rho}{\partial t} + \frac{\partial\rho V\left((1+\epsilon)\rho\right)}{\partial x} = 0 \tag{7}$$

With Equation 4, the following conservation law is obtained:

$$\frac{\partial\rho}{\partial t} + \frac{\partial\rho V\left((1+E(x,\rho))\rho\right)}{\partial x} = 0$$

The kinematic wave solutions of Equation 7 were previously studied (*16*).

New Interpretation of Lane-Changing Intensity Variable

Edie's definition of the average traffic density in a space–time domain A (*20, 21*) is given by

$$\rho(A) = \frac{\sum t_n}{|A|}$$

where t_n is the time for vehicle n in the domain, and $|A|$ is the area of the domain. Following Edie's definition, the effective density is defined by

$$\bar{\rho}(A) = \frac{\sum t_n + t_{nLC}}{|A|} \tag{8}$$

where $t_{n,LC}$ is the lane-changing time of vehicle n in the domain. Therefore, lane-changing intensity in domain A can be defined by

$$\epsilon(A) = \frac{\sum t_{nLC}}{\sum t_n} \tag{9}$$

Thus, lane-changing intensity can be considered the ratio of the total lane-changing time to the total time that vehicles spend in a space–time domain. Here Equation 9 can be considered as an extension of Equation 3, in which the domain is $(x_a, x_b) \times (t_a, t_b)$. With this interpretation, previously developed theories (*16*) are valid for all space–time domains.

DATA SETS AND PREPROCESSING

The present study carefully analyzes lane-changing traffic on a six-lane freeway section on I-80 in Emeryville, near San Francisco, California (Figure 1). Here Lane 1 is a car-pool lane, and there is an on-ramp from Powell Street and an off-ramp to Ashby Avenue. The road section is covered by seven cameras, numbered 1 to 7 from south to north (also the traffic direction); the original videos are transcribed into vehicle trajectories by FHWA's NGSIM project (*22*). Four data sets are available to the public (*23–26*): Data Set 1, with vehicle trajectories of every 15th second on December 3, 2003, from 2:35 to 3:05 p.m.; and Data Sets 2, 3 and 4, with vehicle trajec-

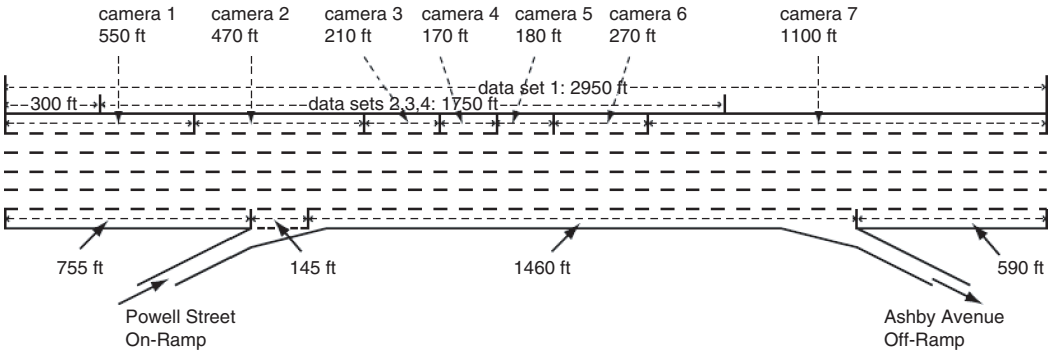

FIGURE 1 I-80 study area.

tories of every 10th second on April 13, 2005, from 4 to 4:15 p.m., 5 to 5:15 p.m., and 5:15 to 5:30 p.m., respectively. The vehicle trajectories are transcribed with different lengths: those in the first data set extend to the downstream Ashby Avenue off-ramp, but not in the other three.

A vehicle at each time instant or frame has 16 describing quantities in the first data set and 18 in the other three data sets. The shared 16 quantities are the identification (ID) of a vehicle (vehicle ID); total number of video frames that the vehicle presents (total frames); the ID of a video frame (frame ID); the elapsed time since January 1, 1970 (global time); lateral distance of the front center of the vehicle from the leftmost edge of the section (local *x*); longitudinal distance of the front center of the vehicle from the entry edge of the section (local *y*); the *x* coordinate of the front center of the vehicle based on California State Plane III in NAD83 (global *x*); the *y* coordinate of the front center of the vehicle based on California State Plane III in NAD83 (global *y*); the length of the vehicle (vehicle length); the width of the vehicle (vehicle width); the class of vehicle (vehicle class: 1 for motorcycles, 2 for autos, and 3 for trucks); instantaneous velocity of the vehicle (vehicle velocity); instantaneous acceleration of the vehicle (vehicle acceleration); the current lane position of the vehicle (lane identification: 1 is the leftmost lane, 6 is the rightmost lane, 7 is the on-ramp from Powell Street, and 8 is the off-ramp to Ashby Avenue); vehicle ID of the leading vehicle in the same lane (preceding vehicle); and vehicle ID of the following vehicle in the same lane (following vehicle). In Data Sets 2 to 4, two additional quantities are used: the spacing between the vehicle and its leader (spacing) and the headway between the vehicle and its leader (headway). The unit of length is feet, and the unit of time is seconds.

The coverage of cameras shown in Figure 1 was determined by playing the videos for Data Set 2 frame by frame. The location of a vehicle is found when its front reaches the end of the region covered by a camera. From the trajectory and video of Vehicle 1, the ends of the regions covered by cameras 1 through 6 in global *y* (local *y*) are 2,133,295 ft (250 ft); 2,133,762 ft (720 ft); 2,133,931 ft (910 ft); 2,134,104 ft (1,080 ft); 2,134,294 ft (1,260 ft); and 2,134,560 ft (1,530 ft), respectively; the on-ramp ends at 2,133,645 ft (605 ft). From the trajectory and video of Vehicle 100, the ends of the regions covered by cameras 1 through 6 in global *y* (local *y*) are 2,133,303 ft (235 ft); 2,133,768 ft (700 ft); 2,133,938 ft (871 ft); 2,134,112 ft (1,048 ft); 2,134,296 ft (1,235 ft); and 2,134,560 ft (1,502 ft), respectively; the on-ramp ends at 2,133,655 ft (586 ft). The errors in the camera coverage are about 10 ft in global *y* and 30 ft in local *y*. From the analysis, the longitudinal distances are subject to measuring errors in the order of 10 ft. The cameras are mounted on high buildings to the east of the road section, and a vehicle's shadow is on its east side. Such a set-up can cause misidentification of vehicles, and errors occur in the lateral direction.

Consistency of Data

In this subsection, the consistency of these data sets is checked. Here Data Set 2 is used as an example: (*a*) the frame IDs of each vehicle in Column 2 are different; (*b*) the total number of frames in Column 3 is correct; and (*c*) each vehicle has a unique length in Column 9, width in Column 10, and class in Column 11. It is also verified that the longitudinal distance from the entry edge of the study section in Column 6 is not decreasing with respect to time for each vehicle, since vehicles are not allowed to travel backward.

It is then verified that the frame ID in Column 2 is consistent with the global time in Column 4. The first frame is at 3:58:55 p.m. on April 13, 2005, of California local time. Since California's time zone is UTC-7 (Coordinated Universal Time) on this day, the first frame corresponds to 10:58:55 p.m. on April 13, 2005, of Greenwich Mean Time. The elapsed time for the first frame since January 1, 1970, equals $9 \cdot 366 + 26 \cdot 365 + (31 + 28 + 31 + 12) = 12{,}886$ days plus 23 h minus 65 s. Thus the first frame's global time is 1,113,433,135,000 ms. For example, the first frame in which Vehicle 1 appears is 12, and the global time is 1,113,433,135,000 + 1,100 = 113,433,136,100 ms. Therefore, the data in Columns 2 and 4 are consistent.

For Data Set 1, a linear relationship can be obtained between local longitudinal coordinates (local *y* in Column 5) and global longitudinal coordinates (global *y* in Column 7) as global *y*:

$$y \approx 2{,}132{,}777.951 + 0.9894 \text{ local } y$$

with *R*-square of 0.99998. For Data Sets 2 to 4 global *y*:

$$y \approx 2{,}133{,}073.377 + 0.9911 \text{ local } y$$

with *R*-square of 0.99995. Thus in the local longitudinal coordinate, the upstream edge in Data Sets 2 to 4 is at about 298 ft in Data Set 1. However, a simple linear relationship cannot be found between local *x* and global *x*. This could be caused by the specific coordinate system used and the special geometric shape of the road section. It also could be caused by measuring errors. Here local lateral coordinates for the study of lane-changing traffic are used. In the data sets, local *x* and *y* correspond to *y* and *x* in the formulations, respectively.

Identification of Lane Changes

This subsection discusses how to extract characteristics of individual lane changes with Data Set 2, for which processed video files were used to verify the results. For the whole data set, all vehicles that occupied two or more lanes are first identified from their lane information, and their classes are distinguished. From the given lane information, 670 vehicles (one motorcycle, 25 trucks, and 644 autos) made lane changes. For each lane change, the vehicle ID, time, longitudinal location, lateral location, previous lane, and target lane are found. For all lane-changing vehicles, the vehicle ID, vehicle class, total number of lane changes, initial lateral location, initial longitudinal location, initial lane, and initial time in the trajectory data set are identified. For Data Set 2, 1,043 lane changes are found: 429 vehicles made one lane change, 158 vehicles made two, 54 vehicles made three, 16 vehicles made four, six vehicles made five, and seven vehicles made six lane changes.

Some lane changes are false due to mistakenly identifying a vehicle's shadow as itself. Such a misidentification usually occurs for vehicles with wide shadows and when they are at the boundaries of cameras. For example, vehicle 1,456, a truck, is misidentified from 448 to 448.5 s when entering the area covered by Camera 3. Since the shadow is to the west of a vehicle, a misidentification results in a lane number that is one greater than the actual lane number. Therefore, two lane changes of the same vehicle are removed if (*a*) they are within 4 s from each other, (*b*) the previous lane of the earlier one is the same as the target lane of the later one, and (*c*) the target lane of the later one is smaller than the previous lane. That is, if a vehicle is swerving to the east and then back in a very short time, it is probably caused by misidentification. For the 1,043 lane changes, 104 such false lane changes are removed, and the removals are randomly verified with video data. Motorcycles, autos, and trucks made two, 82, and 20 of the 104 false lane changes, respectively. For the remaining 939 lane changes, motorcycles, autos, and trucks made zero, 912, and 27 of them, respectively.

Further, 190 lane changes are excluded from Lane 7 to Lane 6, since vehicles do not really change lanes when merging, but only to continue on a new lane. An additional 22 lane changes of mainline vehicles to and from Lane 7 are also excluded. In the final 727 lane changes, 133 are made by 86 on-ramp vehicles, and 594 are made by 451 mainline vehicles. On average, each mainline lane-changing vehicle makes 1.32 lane changes, and each on-ramp lane-changing vehicle makes 1.55 lane changes. In the final 727 lane changes, 23 are made by 16 trucks, and 704 are made by 521 autos. On average, each truck makes 1.44 lane changes, and each auto makes 1.35 lane changes.

For each lane change, the trajectory is extracted as follows. Assume that a lane change occurs at y_{LC}; a threshold of

$$\left(y_{LC}-\frac{\Delta y}{2}, y_{LC}+\frac{\Delta y}{2}\right)$$

is set. This study uses Δy as the width of a vehicle w (between 4.8 and 8.5 ft for vehicles in Data Set 2), or $\frac{1}{2}w$. Then the starting and ending times, x, and y of a lane change are found. It is also assumed that the lane-changing time on each side cannot be longer than 25 s. For Data Set 2, it is found that zero lane changes with lane-changing times greater than 40 s are false, but four lane changes that finish within 10 ft in the longitudinal direction are excluded. The final number of valid lane changes is 723. For Data Set 2, the greatest and smallest angles are 21.38 and 0.10 degrees, respectively; the greatest and smallest lane-changing times are 39.6 and 0.4 s, respectively; and the greatest and smallest speeds are 46.95 and 9.00 mph, respectively.

COMPUTATION OF MACROSCOPIC LANE-CHANGING CHARACTERISTICS

The lane-changing traffic in the weaving section downstream to the on-ramp and upstream to the off-ramp in a space–time domain of $(x_a, x_b) \times (t_a, t_b)$ is considered. Ideally, all vehicles in $(x_a, x_b) \times (t_a, t_b)$ should be detected.

Computation of Density, Speed, and Flow Rate

Figure 2 shows the trajectories on different lanes in the domain of (650, 1,550) × (390, 453) in Data Set 2. Broken trajectories are caused by lane changes.

Assume that N is the number of vehicles in the domain of $(x_a, x_b) \times (t_a, t_b)$. At time t_j, where $j = 1, \ldots, J$, $t_j \in (t_a, t_b)$ and $t_{j+1} - t_j = \Delta t_j = t_b - t_a/J$, the number of vehicles in the region (x_a, x_b), $N([x_a, x_b]; t_j)$ can be found. As shown in Figure 3 for the domain of (650, 1,550) × (201, 264), the dots on the horizontal line show all vehicles in the region at $t_j = 232$ s. Then the average density is

$$\rho\left(\left[x_a, x_b\right] \times \left[t_a, t_b\right]\right) = \frac{\sum_{j=1}^{j} N\left(\left[x_a, x_b\right]; t_j\right)}{J\left(x_b, x_a\right)} \tag{10}$$

Denote the total time that all vehicles spend in the domain $(x_a, x_b) \times (t_a, t_b)$ by $N \cdot T$; then

$$N \cdot T \approx \sum_j N\left(\left[x_a, x_b\right]; t_j\right) = J \cdot \rho\left(\left[x_a, x_b\right] \times \left[t_a, t_b\right]\right) \cdot \left(x_b - x_a\right) \frac{t_b - t_a}{J}$$

$$= \rho\left(\left[x_a, x_b\right] \times \left[t_a, t_b\right]\right) \cdot \left(x_b - x_a\right)\left(t_b - t_a\right)$$

That is, $N \cdot T \approx \rho LT$, where $L = x_b - x_a$, and $T = t_b - t_a$. Thus density is the ratio of vehicles' total travel time to the size of the domain. Therefore, the formula in Equation 10 is an approximation to Edie's definition of traffic density in a space–time domain (*20, 21*), and the approximation error decreases when the number of samples J is increased.

Similarly, the trajectories of vehicles in the domain $(x_a, x_b) \times (t_a, t_b)$ can be sampled at location x_i, where $x_i \in (x_a, x_b)$ and $x_{i+1-} - x_i = \Delta x_i = x_b - x_c/I$, and the average flow rate can be computed by

$$q\left(\left[x_a, x_b\right] \times \left[t_a, t_b\right]\right) = \frac{\sum_{i=1}^{I} N\left(\left[x_a, x_b\right]; t_j\right)}{I\left(t_b - t_a\right)} \tag{11}$$

Thus flow rate can be considered as the ratio of vehicles' total travel distance to the size of the domain, and Equation 11 is an approximation to Edie's definition of flow rate in a space–time domain (*20, 21*). As shown in Figure 3, the dots on the vertical line show all vehicles in the time interval at $x_i = 1{,}100$ ft. Average speed is then computed as

$$v_1\left(\left[x_a, x_b\right] \times \left[t_a, t_b\right]\right) = \frac{q\left(\left[x_a, x_b\right] \times \left[t_a, t_b\right]\right)}{\rho\left(\left[x_a, x_b\right] \times \left[t_a, t_b\right]\right)}$$

The speed for vehicle n in the domain is $v_n = \Delta x_n / \Delta t_n$. The space mean speed is then

$$v_2\left(\left[x_a, x_b\right] \times \left[t_a, t_b\right]\right) = \frac{N}{\sum_{n=1}^{N} \frac{1}{v_n}}$$

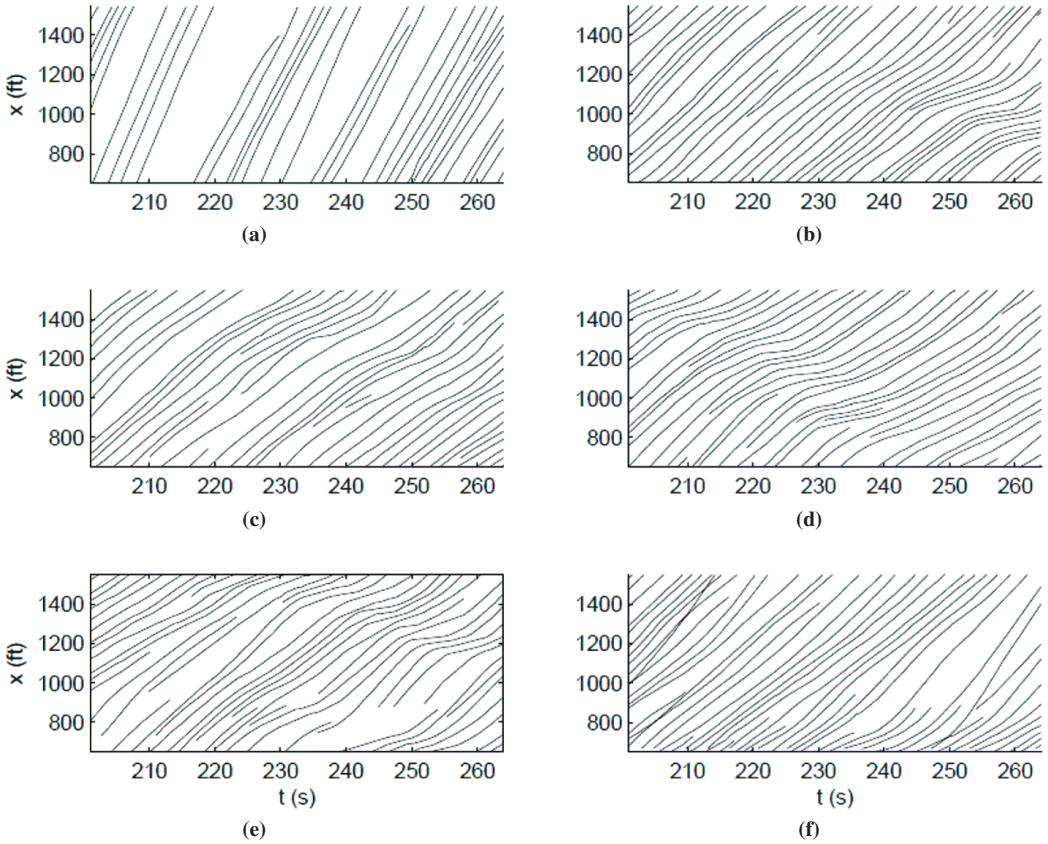

FIGURE 2 Vehicle trajectories in the domain of [650, 1,550] × [390, 453] in Data Set 2: (*a*) Lane 1, (*b*) Lane 2, (*c*) Lane 3, (*d*) Lane 4, (*e*) Lane 5, and (*f*) Lane 6.

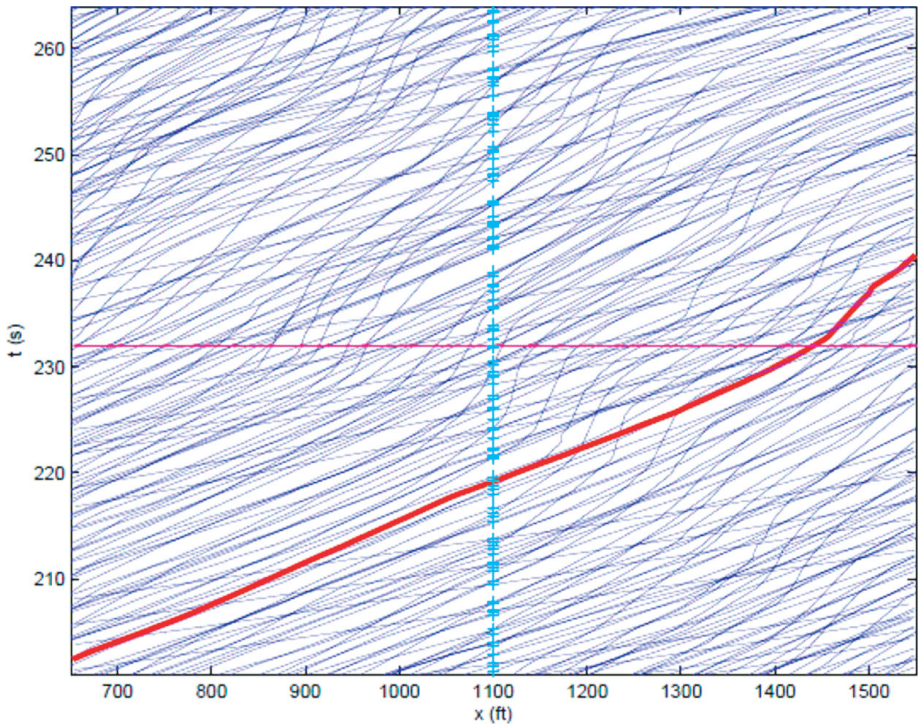

FIGURE 3 Illustration of computation of density, flow rate, and speed.

TABLE 1 Computation of Density, Flow Rate, and Speed for Data Set 2 for Different Time Intervals

$[t_a, t_b]$	75-	138-	201-	264-	327-	390-	453-	516-	579-	642-	705-	768-	831-
ρ	4.33 E+02	4.15 E+02	4.44 E+02	3.83 E+02	4.16 E+02	4.42 E+02	4.81 E+02	4.64 E+02	5.14 E+02	5.18 E+02	4.76 E+02	5.54 E+02	4.74 E+02
SD	4.68 E+01	1.87 E+01	2.00 E+01	3.84 E+01	9.38 E+0	2.02 E+01	5.14 E+01	3.79 E+01	5.80 E+01	4.57 E+01	2.09 E+01	3.53 E+01	3.03 E+01
q	8.16 E+03	8.52 E+03	8.02 E+03	8.43 E+03	9.10 E+03	8.00 E+03	7.48 E+03	8.20 E+03	7.82 E+03	7.87 E+03	8.53 E+03	6.60 E+03	8.39 E+03
SD	4.82 E+02	7.64 E+01	1.55 E+02	1.75 E+02	1.43 E+02	1.86 E+02	2.99 E+02	2.97 E+02	5.59 E+02	4.01 E+02	2.27 E+02	1.45 E+02	1.97 E+02
v_1	18.83	20.53	18.06	22.04	21.90	18.12	15.54	17.66	15.22	15.18	17.92	11.92	17.71
v_2	18.61	20.34	17.18	22.01	21.44	16.84	13.59	17.24	13.59	14.79	17.16	11.05	17.26
$1/v_2$	5.4 E–02	4.9 E–02	5.8 E–02	4.5 E–02	4.7 E–02	5.9 E–02	7.4 E–02	5.8 E–02	7.4 E–02	6.8 E–02	5.8 E–02	9.1 E–02	5.8 E–02
SD	1.6 E–02	1.1 E–02	1.9 E–02	1.2 E–02	1.3 E–02	1.8 E–02	3.8 E–02	1.9 E–02	3.9 E–02	2.3 E–02	1.8 E–02	3.9 E–02	1.5 E–02
v_3	20.47	22.29	20.09	23.89	23.64	19.48	18.53	20.44	17.28	17.14	19.43	14.81	18.99
SD	7.03	9.14	10.07	7.51	8.32	9.87	12.37	10.82	10.14	7.98	8.25	10.49	7.21

and the time mean speed is

$$v_3([x_a, x_b] \times [t_a, t_b]) = \frac{\sum_{n=1}^{N} v_n}{N}$$

Table 1 shows the mean values and standard deviations of density, flow rate, and speed for Data Set 2 for different time intervals. From the table, it is seen that ρ and q are computed more accurately than v_2 and v_3. Thus, hereafter v_1 is used as the average speed, which is consistent with Edie's definition. Generally, $v_2 < v_1 < v_3$. But v_1 is very close to the space mean speed v_2.

Aggregate Characteristics of Lane Changes

Figure 4 shows the trajectories of 30 vehicles in Data Set 2 that made lane changes in the domain of (650, 1550) × (201, 264). The horizontal line shows all lane-changing vehicles in the region at $t = 232$, and with a formula similar to Equation 10 the lane-changing density ρ_{LC} in the domain can be found. The vertical line shows all lane-changing vehicles in the time interval at $x = 1{,}100$ ft, and with a formula similar to Equation 11 the lane-changing flow rate q_{LC} in the domain can be found. In the figure, the solid line is the trajectory for vehicle 576, and the thicker line segment is the trajectory when it is making a lane change. In the model of Equation 3, when vehicle 576 is on the thicker line segment, its contribution to the density should be doubled. Furthermore, the total number of lane changes N_{LC} in the domain, the average lane-changing time t_{LC}, and the total lane-changing time $N_{LC}t_{LC}$ can be found. The average number of lanechanges by each lane-changing vehicle $\alpha = N_{LC}/v_{LC}L$ can also be found.

If a lane change occurs in the space–time domain $(x_a, x_b) \times (t_i, t_i + T)$, it is counted as one lane change in the domain. Thus the number of lane changes N_{LC} is obtained. For all the lane changes, the average angles (θ), the average number of lane changes for each vehicle in the domain, the total time for lane changes $N_{LC}t_{LC}$, and the average lane-changing time t_{LC} can be found. Table 2 shows the mean

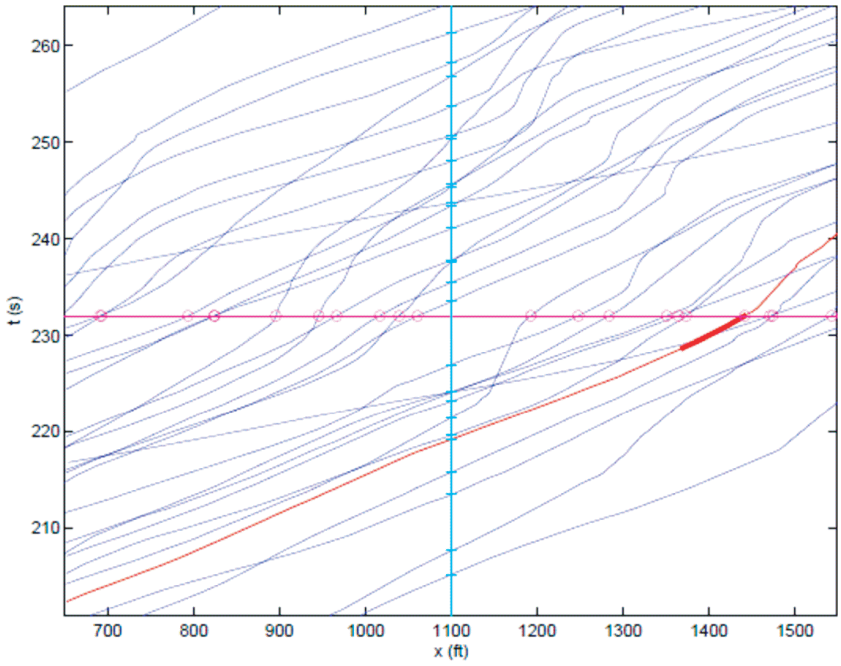

FIGURE 4 Aggregate properties of lane changes.

TABLE 2 Computation of Aggregate Lane-Changing Characteristics for Data Set 2

$[t_a, t_b]$	75-	138-	201-	264-	327-	390-	453-	516-	579-	642-	705-	768-	831-
ρ_{LC}	77.37	59.58	91.30	49.50	50.23	57.66	50.97	57.29	59.22	55.73	74.43	63.98	61.60
SD	22.29	21.07	29.69	15.25	5.00	19.96	11.73	5.51	10.59	7.68	17.86	10.39	17.71
q_{LC}	1.34 E+03	1.14 E+03	1.48 E+03	1.02 E+03	9.93 E+02	9.76 E+02	6.64 E+02	9.59 E+02	7.59 E+02	6.99 E+02	1.14 E+03	6.02 E+02	9.60 E+02
SD	9.21 E+01	1.31 E+02	1.51 E+02	1.37 E+02	7.69 E+01	7.62 E+01	7.56 E+01	6.90 E+01	8.22 E+01	1.14 E+02	2.60 E+02	9.58 E+01	1.12 E+02
θ	5.22	4.52	5.80	3.73	4.52	4.63	4.57	5.66	6.66	5.84	5.66	6.67	5.93
SD	2.80	2.03	3.18	1.80	1.93	1.77	2.38	2.98	4.04	4.16	2.64	2.74	2.56
t_{LC}	3.82	3.39	3.56	4.25	3.69	3.35	6.08	2.68	3.00	5.62	4.15	4.36	3.14
SD	2.28	1.99	3.33	3.10	3.68	2.03	8.83	1.32	1.57	4.59	4.39	4.86	1.54

values and standard deviations of ρ_{LC}, q_{LC}, θ, and t_{LC} for Data Set 2. The standard deviation of t_{LC} could be greater than its mean. For all these values, q_{LC} is the best estimate.

CALIBRATION OF RELATIONSHIP BETWEEN LANE-CHANGING INTENSITY AND TRAFFIC DENSITY

The choice of lane-changing thresholds can significantly affect lane-changing times and, therefore, lane-changing intensity (*16*). But given only vehicles' trajectories, lane-changing thresholds or lane-changing times cannot be accurately told. In the following discussion, lane-changing intensity ϵ is computed according to Equation 3, and $\epsilon = E(x, \rho)$, the relationship between lane-changing intensity and traffic density, is calibrated for different time steps, cell sizes, and locations. The impacts of lane-changing traffic on capacity with Equations 6 and 5 are also discussed.

Different Time Steps

This subsection uses the same road section as in the preceding subsection and sets $\Delta y = w$. First, T is set at 12, 35, 48, and 56 s for four data sets, respectively. From Figure 5, a linear relationship is found between density and lane-changing angle, $\theta = -0.5233 + 0.0122\,\rho$, ($R$-square = .8746). The relationship between density and ϵ, $\epsilon = 0.2251\, e^{-0.0046\,\rho}$ (R-square = .6903), can also be found. From Figure 6, $q = \rho V(\rho)$ has a capacity of 15,316 mph when $\rho = 251$ vehicles per mile (vpm), and $q = \rho V((1 + \epsilon)\rho)$ has a capacity of 13,309 mph

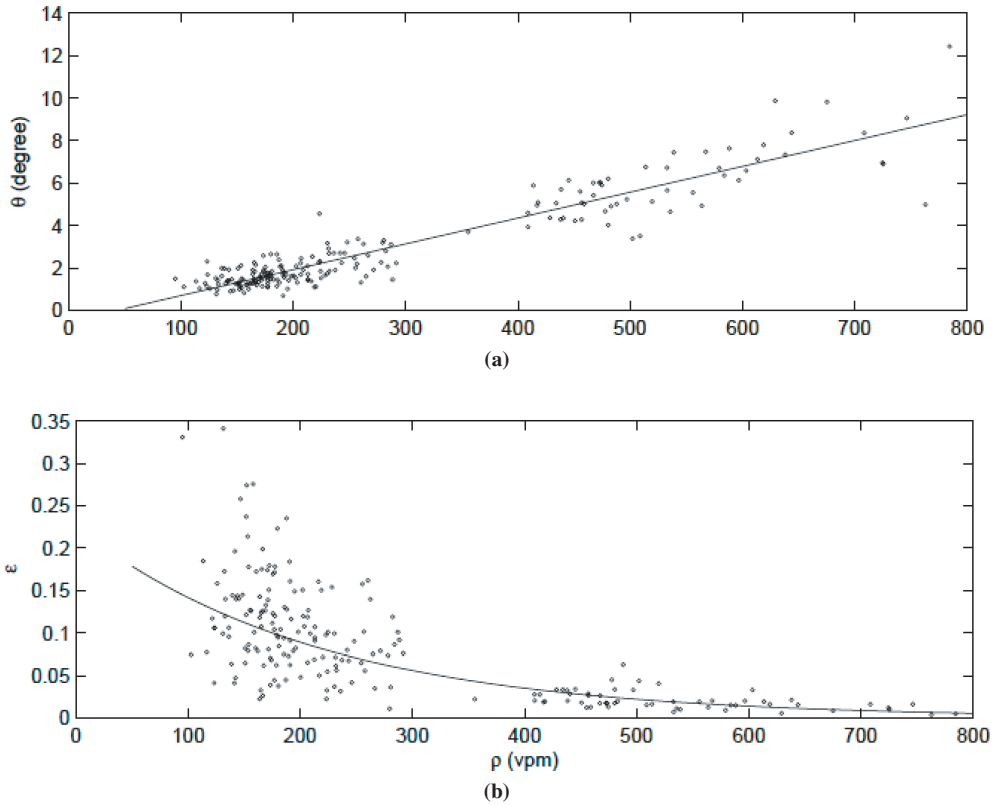

FIGURE 5 Characteristics of lane changes at different densities with T = 12, 35, 48, and 56 s for (*a*) lane-changing angle and (*b*) lane-changing intensity.

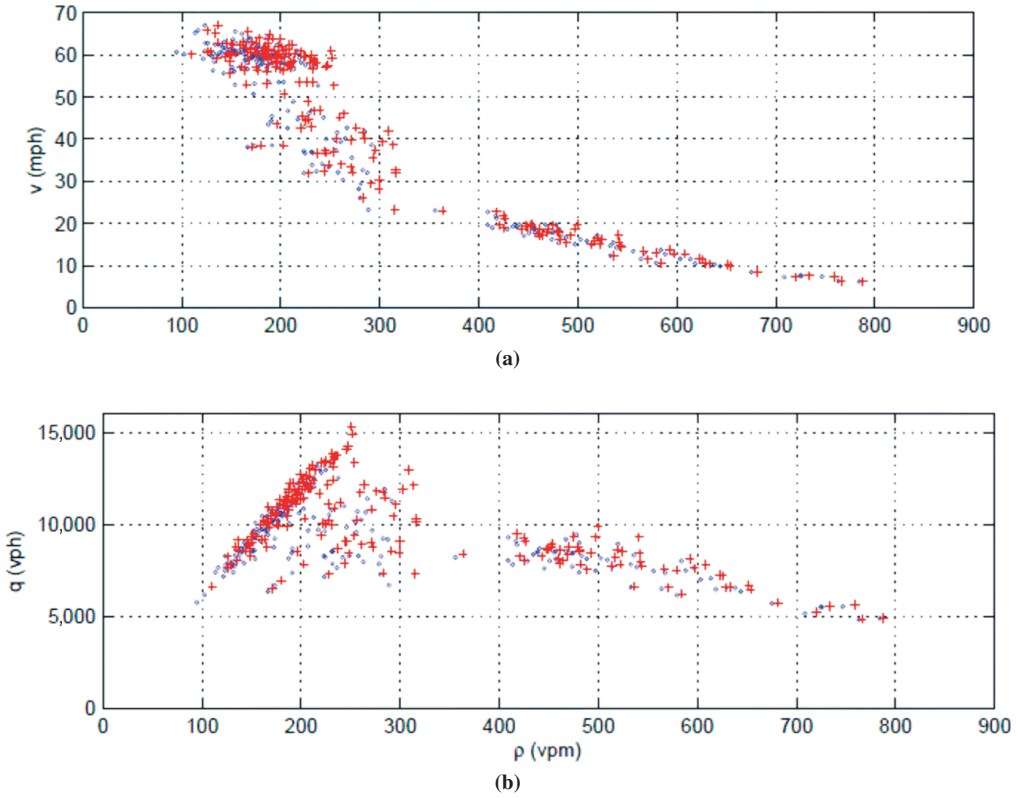

FIGURE 6 Fundamental diagrams with T = 12, 35, 48, and 56 s for (*a*) travel speed and (*b*) flow rate.

when $\rho = 232$ vpm. The lane changes cause a capacity reduction of 13.10%.

With $T = 10$ s for all data sets, the following results. There is a linear relationship between density and lane-changing angle: $\theta = -0.5953 + 0.0126\,\rho$ (R-square = .6421). The relationship between density and ϵ is $\epsilon = 0.2039e^{-0.0044\,\rho}$ (R-square = .5977). Here $q = \rho V(\rho)$ has a capacity of 14,893 mph when $\rho = 253$ vpm, and $q = \rho V((1+\epsilon)\rho)$ has a capacity of 13,520 mph when $\rho = 232$ vpm. The lane changes cause a capacity reduction of 9.22%.

With shorter time intervals T, there are more domains $(x_a, x_b) \times (t_i, t_i + T)$. Different time intervals can yield different results, but both the aggregate lane-changing characteristics and fundamental diagrams are of the same magnitude.

Different Cell Sizes

In this subsection, different road sections downstream to the on-ramp in Figure 1 are considered. First, consider a road section (950, 1400). There is a linear relationship between density and lane-changing angle: $\theta = -0.2633 + 0.0118\rho$ (R-square = .8702). The relationship between density and ϵ is $\epsilon = 0.2116e^{-0.0042\,\rho}$ (R-square = .7630). Here $q = \rho V(\rho)$ has a capacity of 13,231 mph when $\rho = 214$ vpm, and $q = \rho V((1+\epsilon)\rho)$ has a capacity of 12,073 mph when $\rho = 196$ vpm. The lane changes cause a capacity reduction of 8.76%.

Now consider a road section (1,400, 1,850). There is a linear relationship between density and lane-changing angle: $\theta = -0.5967 + 0.0119\rho$ (R-square = .8819); there is also a relationship between density and ϵ: $\epsilon = 0.3074e^{-0.0059\,\rho}$ (R-square = .8040). Now $q = \rho V(\rho)$ has a capacity of 13,807 mph when $\rho = 249$ vpm, and $q = \rho V((1+\epsilon)\rho)$ has a capacity of 12,709 mph when $\rho = 229$ vpm. The lane changes cause a capacity drop of 7.95%.

The results indicate that lane-changing traffic is more active in (950, 1,400) than in (1,400, 1,850). This is as expected, since the former section is immediately downstream to the on-ramp, while the latter is about 500 ft from the on-ramp and 510 ft from the off-ramp.

Different Locations

In this subsection, consider a road section (500, 950) that is upstream to the on-ramp in Figure 1. There is a linear relationship between density and lane-changing angle: $\theta = -0.5921 + 0.0119\rho$ (R-square = .8624). The relationship between density and ϵ is $\epsilon = 0.2570e^{-0.0046\rho}$ (R-square = .8561). Now $q = \rho V(\rho)$ has a capacity of 13,853 mph when $\rho = 251$ vpm, and $q = \rho V((1+\epsilon)\rho)$ has a capacity of 12,301 mph when $\rho = 223$ vpm. The lane changes cause a capacity drop of 11.20%.

Consistent with the results in the preceding subsection, these results indicate that the lane-changing activity is more active in the upstream road section than in the downstream sections.

CONCLUSION

This paper proposes a new interpretation of lane-changing intensity by following Edie's definition of traffic density and extends a macroscopic model of lane-changing traffic flow from the author's previous study. Careful examination of 75 min of vehicle trajectories collected for a freeway section on I-80 is presented. It was found that about 10% misidentified lane changes are caused by long shadows of

vehicles at the boundaries of cameras. For different time intervals, cell sizes, and locations, the well-definedness of the lane-changing intensity variable and intensity–density relation were further verified. It was found that lane-changing angles are highly related to traffic density. Furthermore, lane changes can have significant impacts on the capacity of a multilane road. The observations demonstrate that the new theory can effectively capture the impacts of lane-changing traffic on overall traffic flow without looking into detailed lane-changing mechanisms.

The new definition of lane-changing intensity in Equation 9 will allow the study of lane-changing intensity in other types of space–time domains, for example, along vehicles' trajectories or shock waves. In future studies, the author will be interested in considering the impacts of on- and off-ramp traffic on lane-changing intensities and in determining a reasonable lane-changing threshold. One approach would be to compare capacities of a road section with and without lane changes. However, in the available I-80 data sets, lane-changing activities are quite consistent, and other locations for this task will have to be used. This new macroscopic model of lane-changing traffic is approximate in nature and cannot describe many higher-order characteristics, for example, capacity drops caused by lane changing. The new lane-changing intensity variable and intensity–density relation will have to be verified with other observations. Studying individual vehicles' lane-changing times in different densities will also be of interest. Such studies could shed light on microscopic models of lane-changing traffic.

ACKNOWLEDGMENTS

The author thanks Shin-Ting (Cindy) Jeng and several anonymous reviewers for their valuable comments and discussions.

REFERENCES

1. Hall, F. L., and K. Agyemang-Duah. Freeway Capacity Drop and the Definition of Capacity. In *Transportation Research Record 1320,* TRB, National Research Council, Washington, D.C., 1991, pp. 91–98.
2. Golob, T. F., W. W. Recker, and V. M. Alvarez. Safety Aspects of Freeway Weaving Sections. *Transportation Research Part A,* Vol. 38, No. 1, 2004, pp. 35–51.
3. Gipps, P. G. A Model for the Structure of Lane-Changing Decisions. *Transportation Research Part B,* Vol. 20, No. 5, 1986, pp. 403–414.
4. Yang, Q. *A Simulation Laboratory for Evaluation of Dynamic Traffic Management Systems.* PhD dissertation. Massachusetts Institute of Technology, Cambridge, Mass., 1997.
5. Toledo, T., H. N. Koutsopoulos, and M. E. Ben-Akiva. Modeling Integrated Lane-Changing Behavior. In *Transportation Research Record: Journal of the Transportation Research Board, No. 1857,* Transportation Research Board of the National Academies, Washington, D.C., 2003, pp. 30–38.
6. Kesting, A., M. Treiber, and D. Helbing. General Lane-Changing Model MOBIL for Car-Following Models. In *Transportation Research Record: Journal of the Transportation Research Board, No. 1999,* Transportation Research Board of the National Academies, Washington, D.C., 2007, pp. 86–94.
7. Michalopoulos, P. G., D. E. Beskos, and Y. Yamauchi. Multilane Traffic Flow Dynamics: Some Macroscopic Considerations. *Transportation Research Part B,* Vol. 18, No. 4–5, 1984, pp. 377–395.
8. Holland, E. N., and A. W. Woods. A Continuum Model for the Dispersion of Traffic on Two-Lane Roads. *Transportation Research Part B,* Vol. 31, No. 6, 1997, pp. 473–485.
9. Daganzo, C. F. A Behavioral Theory of Multi-Lane Traffic Flow. Part I: Long Homogeneous Freeway Sections; Part II: Merges and the Onset of Congestion. *Transportation Research Part B,* Vol. 36, No. 2, 2002, pp. 131–169.
10. Coifman, B. Estimating Density and Lane Inflow on a Freeway Segment. *Transportation Research Part A,* Vol. 37, No. 8, 2003, pp. 689–701.
11. Gazis, D. C., R. Herman, and G. H. Weiss. Density Oscillations Between Lanes of a Multilane Highway. *Operations Research,* Vol. 10, No. 5, 1962, pp. 658–667.
12. Munjal, P. K., and L. A. Pipes. Propagation of On-Ramp Density Waves on Uniform Unidirectional Multilane Freeways. *Transportation Research,* Vol. 5, 1971, pp. 241–255.
13. Jin, W.-L., Y. Zhang, and L. Chu. Measuring First-In-First-Out Violation Among Vehicles. Presented at 85th Annual Meeting of the Transportation Research Board, Washington, D.C., 2006.
14. Leisch, J. E. A New Technique for Design and Analysis of Weaving Sections on Freeways. *ITE Journal,* Vol. 49, No. 3, 1979, pp. 26–29.
15. Laval, J. A., and C. F. Daganzo. Lane-Changing in Traffic Streams. *Transportation Research Part B,* Vol. 40, No. 3, 2006, pp. 251–264.
16. Jin, W.-L. A Kinematic Wave Theory of Lane-Changing Traffic Flow. *Transportation Research Part B,* Vol. 44, No. 8–9, 2010, pp. 1001–1021.
17. Greenshields, B. D. A Study in Highway Capacity. *Highway Research Board Proceedings,* Vol. 14, 1935, pp. 448–477.
18. Lighthill, M. J., and G. B. Whitham. On Kinematic Waves: II. A Theory of Traffic Flow on Long Crowded Roads. *Proceedings of the Royal Society of London A,* Vol. 229, No. 1178, 1955, pp. 317–345.
19. Richards, P. I. Shock Waves on the Highway. *Operations Research,* Vol. 4, No. 1, 1956, pp. 42–51.
20. Edie, L. C. Discussion on Traffic Stream Measurements and Definitions. In *Proceedings of Organisation for Economic Co-operation and Development,* 1965.
21. Cassidy, M. J., and B. Coifman. Relation Among Average Speed, Flow, and Density and Analogous Relation Between Density and Occupancy. In *Transportation Research Record 1591,* TRB, National Research Council, Washington, D.C., 1997, pp. 1–6.
22. FHWA. *Next Generation SIMulation Fact Sheet.* Technical report. FHWA-HRT-06-135. 2006.
23. Cambridge Systematics, Inc. *NGSIM BHL Data Analysis.* Technical report. Summary report prepared for FHWA, 2004.
24. Cambridge Systematics, Inc. *NGSIM I-80 Data Analysis (4:00 p.m. to 4:15 p.m.).* Technical report. Summary report prepared for FHWA, 2005.
25. Cambridge Systematics, Inc. *NGSIM I-80 Data Analysis (5:00 p.m. to 5:15 p.m.).* Technical report. Summary report prepared for FHWA, 2005.
26. Cambridge Systematics, Inc. *NGSIM I-80 Data Analysis (5:15 p.m. to 5:30 p.m.).* Technical report. Summary report prepared for FHWA, 2005.

The views and results are the author's alone.

The Traffic Flow Theory and Characteristics Committee peer-reviewed this paper.